Congenital Skeletal Dysplasias: Imaging Pitfalls

42

Richa Arora and Kakarla Subbarao

Contents

R. Arora, MD, MMed, FRCR (✉) • K. Subbarao, FRCR, FACR, FICP, FCCP, FICR
Department of Radiology & Imageology, Nizam's Institute of Medical Sciences,
Punjagutta, Hyderabad, Telangana 500082, India
e-mail: dr.richaarora@gmail.com;
subbaraokakarla25@gmail.com

42.1 Introduction

Skeletal dysplasias (or osteochondrodysplasias) comprise of a large heterogeneous group of disorders of the bone or cartilage growth, which continue to evolve throughout life and are due to genetic mutations. Thus, they differ from dysostosis which can be defined as malformation of single or multiple bones occurring due to abnormal blastogenesis *in utero* and which remain phenotypically static throughout life (Resnick 1994; Yochum and Rowe 2005). There are 450 different dysplasias mentioned in the literature (Warman et al. 2011), and various epidemiologic studies have reported their overall prevalence of 2.3–7.6 per 10,000 births (Rasmussen et al. 1996). Majority of these disorders are confusing and have overlapping features with the other entities. It is important to be familiar with their imaging features and those of various other radiologically similar dysplasias and non-dysplastic pathologies, to aid in their accurate diagnosis and for early institution of the appropriate therapy, prognostication, and counseling of the family regarding inheritance pattern and risk of recurrence. This would also prevent serious sequelae or com-

plications associated with some of these dysplasias. This chapter focuses on the imaging mimics found in commonly encountered skeletal dysplasias.

42.2 Thanatophoric Dysplasia and Achondrogenesis

Thanatophoric dysplasia is the second most common lethal dysplasia (the most common is osteogenesis imperfecta type 2). It is characterized by marked short-limbed dwarfism with bowing of tubular bones, macrocephaly with frontal bossing, small thoracic cage, and severe platyspondyly (Yochum and Rowe 2005). The vast majority of cases are due to sporadic mutations coding for the fibroblast growth receptor 3 (FGFR3) located in chromosome 4p16.3. Patients often die within the first 48 h of birth, either from pulmonary hypoplasia caused by a narrow thorax or brain stem and cervical cord compression from foramen magnum stenosis. It has two subtypes (Miller et al. 2009). The typical radiographic features (Fig. 42.1) include macrocephaly with frontal bossing (with cloverleaf skull appearance in type II), narrow chest with short horizontal ribs, small scapulae, marked platyspondyly with flattening of the vertebral bodies and widened disk spaces against a backdrop of well-formed neural arches giving the "H" or "inverted U" appearance (on frontal radiograph of the spine), relatively normal trunk length, small squared iliac wings with horizontal acetabular roofs and small sacrosciatic notches, shortening of proximal portions of long limbs (rhizomelia), and bowing of long tubular bones (commonly humeri and femurs) giving the "telephone handle" appearance with metaphyseal flaring (in type I). Clinically, these fetuses have flat facies with a depressed nasal bridge and proptosis (Keats et al. 1970; Kozlowski et al. 1970; Miller et al. 2009).

Achondrogenesis is another lethal type of osteochondrodysplasia characterized by poor or deficient ossification of the vertebral column, sacrum, and pelvic bones and shortening of tubular bones (but this is quite rare). It is divided into

Fig. 42.1 Babygram of a fetus with thanatophoric dysplasia shows severe platyspondyly with well-formed neural arches (giving a "H"-shaped appearance), narrow and elongated chest (normal trunk length), small squared iliac bones, shortening of tubular bones with bowing deformity (telephone handle deformity, particularly in bilateral femurs and humeri), and relatively large skull (Courtesy of Dr. Hani Al Salam with permission from Radiopaedia. org)

two types, and type I (which is more severe and is associated with multiple rib fractures and involvement of the hands) has further two subtypes. Type I is caused by recessive mutation in the DTDST gene (responsible for encoding the diastrophic dysplasia sulfate transporter), and type II is caused by the dominant mutation in the COL2A1 gene. Although all types are lethal, type II has fewer stillbirths, longer survival, and relatively larger baby with longer limbs (Kapur 2007). The characteristic imaging features (Fig. 42.2) include short tubular bones (more pronounced in type I) with metaphyseal flaring and spurring (resembling thorn apples), poor or absent ossification of carpals and phalanges, poor

Fig. 42.2 Babygram of a fetus with achondrogenesis shows poor ossification of the vertebral column (with ossified pedicles) and pelvis, narrow chest with short horizontal ribs, small scapulae, markedly shortened bilateral femurs with metaphyseal flaring and spurring, and relatively large skull (Reproduced with permission from: Subbarao (2014))

or deficient ossification of the vertebral column with pedicles generally ossified, narrow thorax with short ribs (ribs are thin and show multiple

fractures in type IA), pulmonary hypoplasia, small iliac bones (with only upper portion ossified in type IA) with poor ossification of the ischium, normal-sized skull (which appears relatively large compared to hypoplastic skeleton and with poor ossification in type I), and micrognathia. Antenatal ultrasound (US) imaging may show polyhydramnios and hydrops fetalis (Kapur 2007).

Both these entities have common features of poorly ossified spine (with posterior elements generally well formed), narrow thorax, shortened tubular bones, and small pelvis. However, the presence of short trunk with narrow thorax (in contrast to narrow and elongated thorax in thanatophoric dysplasia), marked shortening of tubular bones without bowing deformity, rib fractures, micrognathia, and polyhydramnios and hydrops fetalis favor achondrogenesis. Cloverleaf skull, if present, suggests thanatophoric dysplasia (Keats et al. 1970; Kozlowski et al. 1970; Kapur 2007; Miller et al. 2009).

42.3 Chondroectodermal Dysplasia and Jeune Syndrome

Chondroectodermal dysplasia (also known as Ellis-van Creveld syndrome) is a rare autosomal recessive skeletal dysplasia, which belongs to the short-rib dysplasia group of osteochondrodysplasias and is due to mutation affecting the EVC gene on locus 4p160 (Baujat and Le Merrer 2007). It is characterized by the involvement of ectoderm along with the skeleton and was first described by Richard WB Ellis and Simon van Creveld in 1940 (Chauss 1955). This condition manifests at birth with characteristic features of disproportionate short-limb dwarfism; dysplastic nails, teeth, and hair; postaxial polydactyly (hexadactyly); multiple labiogingival frenula; congenital cardiac defects (most common being single atrium and atrioventricular cushion defects); cryptorchidism; and epispadias. The imaging features (Fig. 42.3) include narrowing of the thorax with short ribs, progressive acromeso-
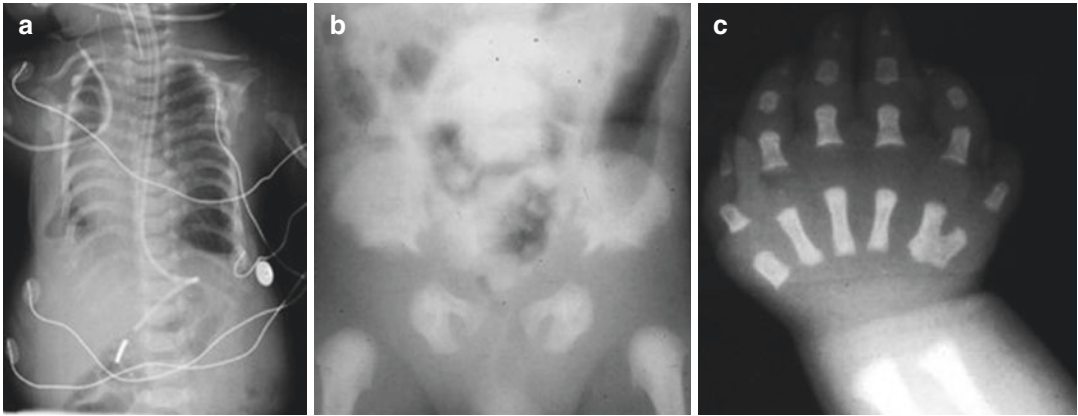
Fig. 42.3 Chondroectodermal dysplasia. (**a**) Frontal chest radiograph shows narrowing of the thorax with short horizontal ribs. (**b**) Frontal radiograph of the pelvis shows short flared iliac wings with trident acetabula. (**c**) Frontal radiograph of the hands shows postaxial polydactyly with fusion of the fifth and sixth metacarpals and disproportionate shortening of middle and distal phalanges (Courtesy of Dr. Radswiki with permission from Radiopaedia.org)

Fig. 42.4 Jeune syndrome. (**a**) Frontal chest radiograph shows short horizontal ribs with a narrow thorax. (**b**) Radiograph of the pelvis shows small flared iliac bones with trident acetabula (same as in chondroectodermal dysplasia) (Courtesy of Dr. Radswiki with permission from radiopaedia.org)
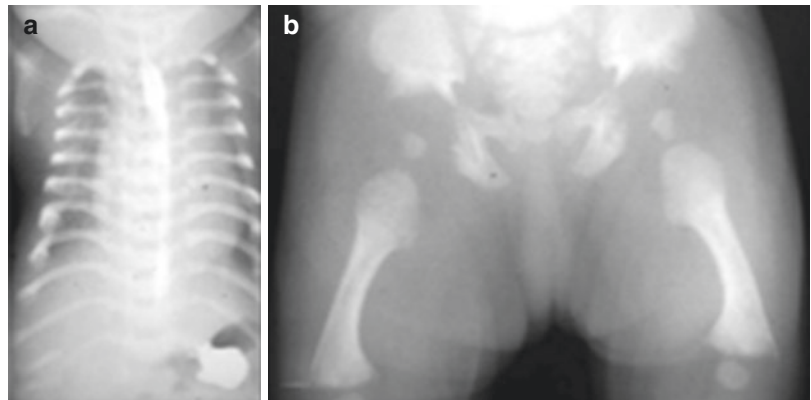
melia (shortening of distal and middle segments as opposed to proximal segments – involving forearms and lower legs – and disproportionate shortening of distal and middle phalanges in the hands), postaxial hexadactyly in the hands and sometimes in the toes, carpal fusion involving the capitate and hamate, cone-shaped epiphysis of phalanges of the hands, premature ossification of femoral capital epiphysis, hypoplastic lateral proximal tibial epiphysis, genu valgum, short pelvis with flared iliac wings and narrow base, and trident acetabula (horizontal acetabular roof with three downward-projecting spikes). The differential diagnosis includes asphyxiating thoracic dysplasia and other short-rib syndromes (with or without polydactyly) (Chauss 1955; Baujat and Le Merrer 2007; Weiner et al. 2013).

Jeune syndrome (or asphyxiating thoracic dystrophy) is another autosomal recessive short-rib dysplasia with a severely narrow thorax. The imaging features are almost same (Fig. 42.4) as those seen in chondroectodermal dysplasia except that it can be differentiated by the absence of involvement of ectodermal structures (such as the hair, nail, and teeth), lack of cardiac anomalies, absence of both carpal fusion, and hypoplastic lateral proximal tibial epiphysis. Unlike chondroectodermal dysplasia, polydactyly is seen rarely in Jeune syndrome, and involvement of the thorax is more severe (Chauss 1955; Baujat

and Le Merrer 2007; de Vries et al. 2009; Tüysüz et al. 2009; Thakkar et al. 2012; Weiner et al. 2013). Additional manifestations, including liver fibrosis, cystic renal dysplasia, cystic pancreatic disease, and retinal pigmentary degeneration, have also been described in some cases of Jeune syndrome (de Vries et al. 2009; Tüysüz et al. 2009; Thakkar et al. 2012).

42.4 Osteogenesis Imperfecta, Non-accidental Injury, Rickets, Hypophosphatasia, and Juvenile Idiopathic Osteoporosis

Osteogenesis imperfecta (OI) (also known as brittle bone disease) is a genetic disorder of collagen type I production (involving connective tissues and bones) due to mutations in either the COL1A1 or the COL1A2 gene. The clinical features are variable – based on its subtype – and include osteoporosis, increased bone fragility, blue sclera, dental fragility, and hearing loss (Renaud et al. 2013; Greenspan 2015). The hallmarks on imaging (Fig. 42.5) include osteopenia, bone fractures, and bone deformities. Osteopenia occurs due to cortical bone thinning and trabecular bone rarefaction. Bone densitometry by dual-energy X-ray absorptiometry (DXA) is the appropriate method to detect decreased bone mineral density. However, it is important to exclude other entities such as rickets, hypophosphatasia, and juvenile idiopathic osteoporosis (and rarely prematurity, leukemia, hypogonadism, growth hormone deficiency, hyperthyroidism, juvenile diabetes mellitus) causing reduced bone mineral density. Fractures can involve the axial and appendicular skeleton and often involve diaphysis of long bones with exuberant callus formation. Vertebral compression fractures and spondylolysis of L5 vertebra are also seen. Bone deformities occur due to excessive bone malleability and plasticity and include deformed gracile over-tubulated bones with diaphyseal bowing and angulation, basilar invagination, codfish vertebrae, platyspondyly, kyphoscoliosis, pectus carinatum or excavatum, protrusio acetabuli, and
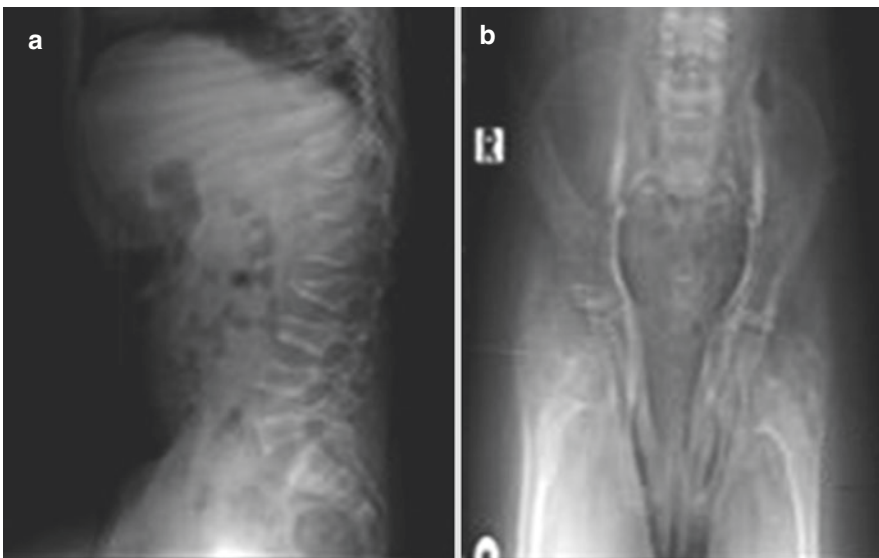
Fig. 42.5 Osteogenesis imperfecta. (**a**) Lateral radiograph of the thoracolumbar spine shows osteopenia with thin cortices, codfish vertebrae in the lumbar spine, and compression fractures with anterior wedging involving the L1 and L2 vertebrae. (**b**) Frontal radiograph of the pelvis shows osteopenia and triangular pelvis with bilateral protrusio acetabuli. (**c**, **d**) Frontal radiographs of both femurs show osteopenia with bowing deformities

Fig. 42.5 (continued)

coxa vara. Other features include wormian bones, popcorn calcification in the metaphyses and epiphyses (especially in the knee) due to micro-traumatic fragmentation and disordered matura-tion of the growth plate, ossification of the interosseous membrane, and dense metaphyseal bands leading to the zebra stripe sign (in children receiving bisphosphonates) (Renaud et al. 2013; Greenspan 2015). It is difficult to diagnose milder forms of OI (types I and IV) especially in cases with negative family history and with no obvious extraskeletal manifestations.

Non-accidental injury (NAI) is an important differential in young children. Nevertheless, cer-tain features, namely, fractures of varying ages,

no evidence of osteopenia, peculiar fractures (such as metaphyseal corner fractures (Fig. 42.6), posterior rib fractures, and complex skull frac-tures), subdural hematomas, retinal hemorrhage, absence of wormian bones, and modeling defor-mities, favor NAI (Ablin et al. 1990). *Rickets* and *hypophosphatasia* are other differentials as they show defective skeletal mineralization, bone fractures, and deformities. Hypophosphatasia is a rare autosomal recessive metabolic disorder characterized by a reduced tissue-nonspecific isoenzyme of alkaline phosphatase (TNSALP) and increased urinary excretion of phosphoetha-nolamine. However, the presence of metaphyseal changes (cupping, fraying, and splaying with

Fig. 42.6 Non-accidental injury. Frontal radiograph of the tibia and fibula shows a distal metaphyseal corner fracture in the tibia along with the periosteal reaction. Bone density is normal

Fig. 42.7 Rickets. Frontal radiograph of both knees shows osteopenia with bowing deformity resulting in knock-knees. Additionally, metaphyseal changes in the form of splaying, fraying, cupping, and widened growth plates are also seen

widened growth plate) (Fig. 42.7) and presence of biochemical changes help in differentiating both these entities from OI (Grover et al. 2003). *Idiopathic juvenile osteoporosis* is a rare sporadic disorder which manifests with pain in bones, osteoporosis, fractures, and deformity of the axial and appendicular skeleton (Fig. 42.8), often between 2 and 14 years of age. Diagnosis is established by excluding other causes of osteoporosis (normal biochemical findings and negative findings on hormone assays), negative family history, and in an appropriate clinical setting, with no features of hearing loss or blue sclera.

Fractures often involve vertebrae and metaphysis of long bones (Imerci et al. 2015).

42.5 Osteopetrosis, Pyknodysostosis, and Cleidocranial Dysostosis

Osteopetrosis (also known as marble bones or Albers-Schonberg disease) is a rare hereditary disorder which occurs due to defective osteoclasts, resulting in lack of resorption of primitive osteochondrous tissue, leading to diffusely sclerotic and brittle bones. It has three subtypes: benign autosomal dominant form, severely malignant autosomal recessive form, and an intermediate recessive type with renal tubular acidosis (Machado et al. 2015). Radiographic features (Fig. 42.9) include diffuse increase in bone density without trabeculation

Fig. 42.8 Juvenile idiopathic osteoporosis. Lateral radiograph of the thoracolumbar shows osteopenia with thin cortices and multiple compression fractures (Courtesy of Dr. Anwar Adil, Karachi X-rays CT and Ultrasound Centre, Pakistan)

and with loss of cortical and medullary differentiation; bone-within-a-bone appearance (also known as endobones that represent fetal vestiges which are normally removed) particularly involving innominate bones, calcaneum, and ribs; multiple transverse fractures (banana fractures) with abundant callus formation; failure of metaphyseal remodeling resulting in "Erlenmeyer flask" deformity (see Table 42.1 for list of differentials); uniformly sclerotic vertebrae or dense bands adjacent to vertebral end plates giving the appearance of "sandwich vertebrae;" sclerosis of calvarial vault and base of the

skull; and poor pneumatization of the paranasal sinuses. In type III osteopetrosis (associated with tubular acidosis), rachitic changes are an additional finding (Resnick 1994; Machado et al. 2015). Complications include pathological fractures, hydrocephalus, cranial nerve palsies, optic atrophy, deafness, dental caries secondary to faulty dentition, anemia, infections, leukemia, and sarcoma (Resnick 1994; Yochum and Rowe 2005; Machado et al. 2015).

Pyknodysostosis is also known as *Toulouse-Lautrec syndrome*, named after the French painter who was affected with this disease. It is a rare autosomal recessive, lysosomal disorder with abnormal osteoclast function due to genetic deficiency in cathepsin K which has been mapped to chromosome 1q21, leading to increase in bone density. It is a hybrid between osteopetrosis and cleidocranial dysostosis and shares its imaging features with both. It presents in early childhood with short stature (Resnick 1994; Bathi and Masur 2000). The main radiological abnormality (Figs. 42.10 and 42.11) is generalized osteosclerosis with preservation of medullary canal (unlike osteopetrosis, in which medullary canal is encroached upon, resulting in anemia and extramedullary hematopoiesis). The osteosclerosis is most pronounced in the limbs, followed by the clavicles, mandible, skull, and spine. Another major feature mimicking osteopetrosis is the presence of transverse fractures in the long bones. However, metaphyseal remodeling is normal. Other features which are exclusively seen in pyknodysostosis and differentiate it from osteopetrosis (Table 42.2) include marked delay in sutural closure, persistent fontanelles, wormian bones, frontoparietal bossing, nasal beaking, obtuse mandibular gonial angle often with relative prognathism, persistence of deciduous teeth, clavicular hypoplasia, and, lastly, aplasia of terminal phalanges simulating acro-osteolysis. Platybasia and vertebral segmentation anomalies (spool-shaped vertebrae) are also common, particularly at the craniovertebral and lumbosacral regions. Osteomyelitis of the jaw is a frequent complica-
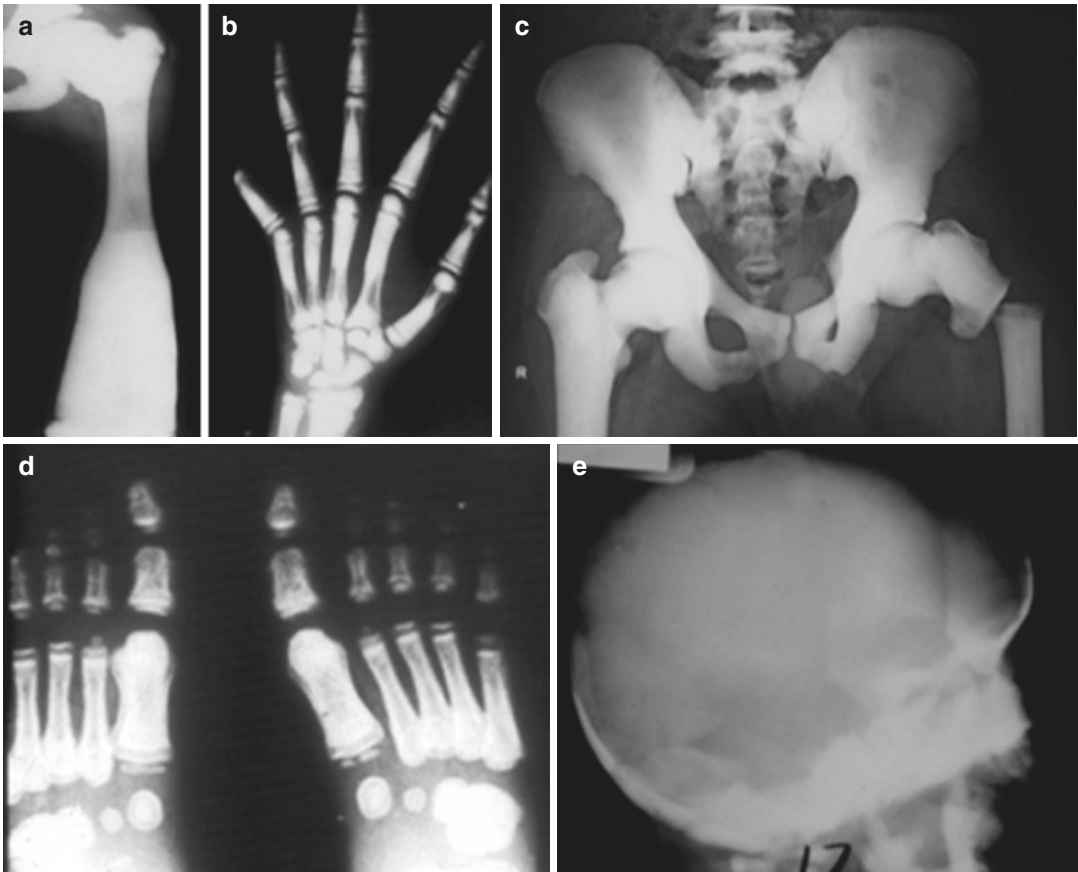
Fig. 42.9 Osteopetrosis. (**a**) Frontal radiograph of the femur shows osteosclerosis with abnormal distal metaphyseal remodeling resulting in the "Erlenmeyer flask" deformity. (**b**) Frontal hand radiograph shows the "bone-within-a-bone" appearance (endobones) along with increased bone density. (**c**) Frontal radiograph of the pelvis shows osteosclerosis with obliteration of the trabeculae along with "banana" type of fracture in the left proximal femur. (**d**) Frontal radiograph of both feet shows generalized increased bone density. (**e**) Lateral skull radiograph shows sclerosis of the base of the skull with no evidence of widened sutures/fontanelles or wormian bones (Reproduced with permission from: Subbarao (2013))

Table 42.1 Erlenmeyer flask deformity: causes and differentiating features

| Etiology	Other characteristic features
Osteopetrosis	Diffuse osteosclerosis, transverse fractures with abundant callus, bone-within-a-bone appearance, sandwich vertebrae, other manifestations
Pyle disease	Lucent and flask-shaped metaphysis with narrow and sclerotic shafts
Thalassemia	Coarsened trabeculations producing a "cobweb" appearance
Niemann-Pick and Gaucher disease	Osteopenia with thin cortices, avascular necrosis of bones, hepatosplenomegaly
Lead poisoning	Dense metaphyseal bands
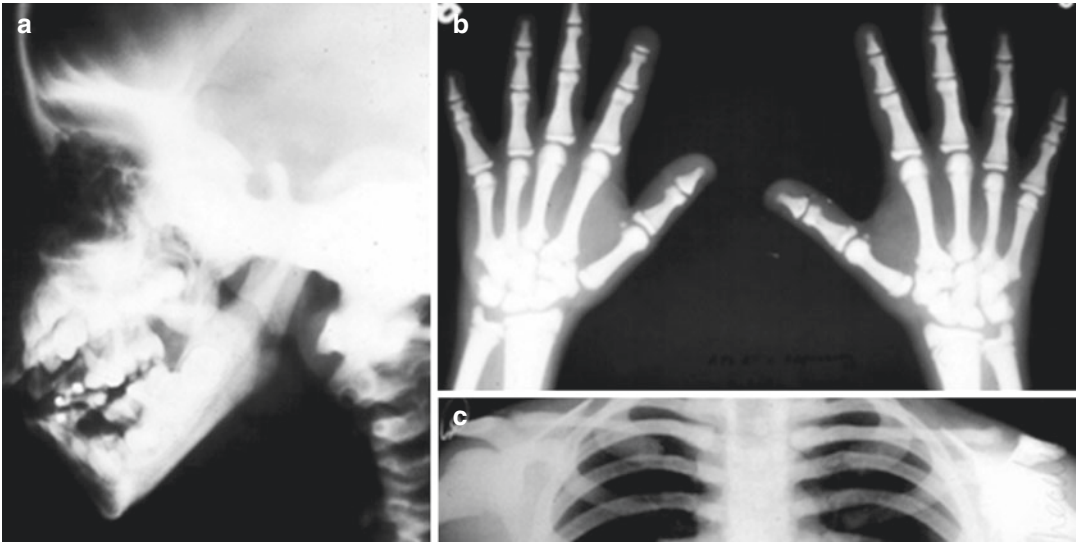
Fig. 42.10 Skeletal survey in a patient with pyknodysostosis. (**a**) Oblique radiograph of the mandible shows osteosclerosis with obtuse angle of the mandible. (**b**) Frontal radiograph of both hands shows terminal phalangeal hypoplasia mimicking acro-osteolysis (apart from osteosclerosis). (**c**) Frontal radiograph of both clavicles shows hypoplasia of the lateral aspect of the left clavicle and the junction of medial one-third and lateral two-thirds of the right clavicle (Reproduced with permission from: Subbarao (2013))
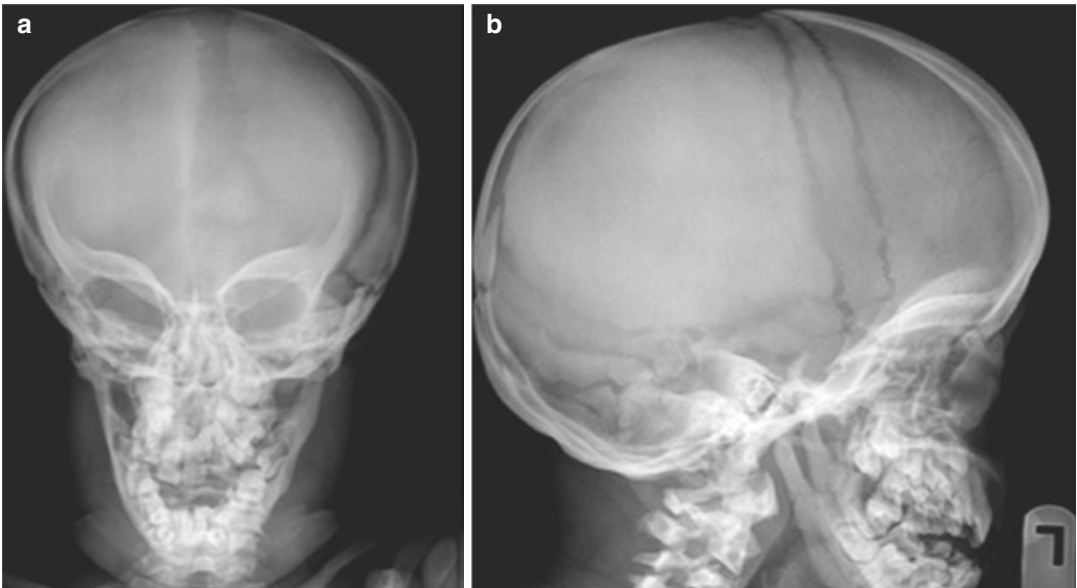

Fig. 42.11 Pyknodysostosis. (**a**) Frontal and (**b**) lateral skull radiographs show widened sutures and wormian bones, apart from osteosclerosis (Courtesy of Dr. Mark Holland with permission from Radiopaedia.org)

Table 42.2 Imaging pitfalls and differentiating features between osteopetrosis and pyknodysostosis

Imaging pitfalls	Osteopetrosis (exclusive features)	Pyknodysostosis (exclusive features)
Generalized osteosclerosis and transverse fractures in the bones	Obliteration of trabeculae and involvement of medullary canal leading to anemia and extramedullary hematopoiesis	Medullary canal is spared
	Erlenmeyer flask deformity in the long bones Bone-within-a-bone appearance Sandwich vertebrae	Delay in suture closure and persistent fontanelles Wormian bones Obtuse angle of the mandible Clavicle hypoplasia Terminal phalangeal aplasia mimicking acro-osteolysis

tion (Resnick 1994; Bathi and Masur 2000; Yochum and Rowe 2005).

Cleidocranial dysostosis is a rare non-sclerosing, autosomal dominant skeletal dysplasia predominantly affecting development of intramembranous and enchondral bones. It is caused by mutation in CBFA1 gene on chromosome 6. Skull and clavicular anomalies and incomplete ossification of midline skeletal structures are classic hallmarks of this entity. The typical clinical features are large head, small face, and excessively mobile drooping shoulders. Dwarfism is not present though height is slightly reduced in the affected patients (Shen et al. 2009). The radiographic features (Fig. 42.12) include delayed ossification of the calvaria, widening of skull sutures (sagittal and coronal) and persistent fontanelles, wormian bones, persistent metopic suture, frontoparietal bossing/brachycephaly, underdeveloped facial bones including nasal bone and the maxilla with hypoplastic paranasal sinuses, large mandible, delayed and defective dentition, hypoplasia/aplasia of lateral clavicle, small and elevated scapulae, narrow and bell-shaped chest, pseudo-widening of the symphysis pubis (due to absent/delayed ossification of the pubic bones), delayed mineralization of the vertebrae along with segmentation anomalies in the spine, and hypoplastic radius and fibula (Shen et al. 2009). The pitfalls and the differentiating features from pyknodysostosis are tabulated in Table 42.3.

42.6 Morquio and Hurler Syndromes and Spondyloepiphyseal Dysplasia Tarda

Morquio syndrome is an autosomal recessive type IV mucopolysaccharidosis (MPS), which occurs due to deficiency of N-acetyl galactosamine-6-sulfatase resulting in excess accumulation of the keratan sulfate in the various tissues, particularly the cartilage, nucleus pulposus of intervertebral disks, and cornea. Diagnosis is established by keratosulphaturia, which differentiates it from Hurler syndrome. Patients present in the early childhood with features of short-trunk dwarfism, thoracolumbar kyphosis, protuberant sternum, and deafness. The mental capacity in the affected patients is normal, unlike Hurler syndrome (Langer and Carey 1966; Mikles and Stanton 1997; Di Cesare et al. 2012). Radiological features (Fig. 42.13) include universal platyspondyly with anterior central vertebral beaking and posterior scalloping, round vertebra, posteriorly displaced and hypoplastic L1 or L2 vertebra, normal or increased disk heights, odontoid hypoplasia, atlantoaxial subluxation, goblet-shaped flared iliac wings, hypoplastic acetabuli, flattened capital femoral epiphysis, unstable hip, coxa vara or valga, short and wide tubular bones with or without metaphyseal flaring, proximal metacarpal tapering, hand and foot deformities, pectus carinatum,
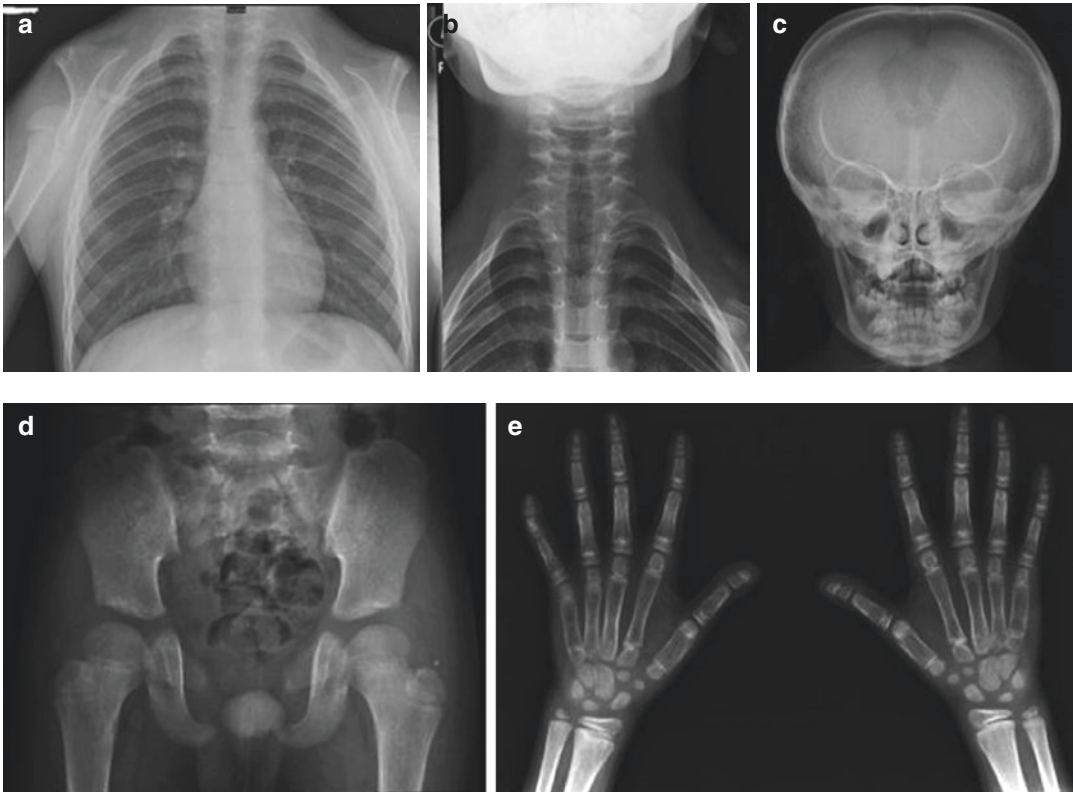
Fig. 42.12 Cleidocranial dysplasia. (**a**) Frontal chest radiograph shows the absence of both clavicles with omovertebral bones articulating with the T3 transverse processes on both sides, bell-shaped chest, small and high scapulae, and non-visualization of both glenoid fossa with inferiorly located humeral heads. (**b**) Frontal radiograph of the cervicothoracic spine shows bifid C7 to T2 vertebrae. (**c**) Frontal skull radiograph shows widened anterior and posterior fontanelles, wormian bones, and a large mandible. (**d**) Frontal radiograph of the pelvis shows diastasis of the pubic symphysis, hypoplastic iliac bones, and bilateral short femoral necks causing coxa vara deformity. (**e**) Frontal radiograph of both hands shows an elongated second metacarpal bone and hypoplastic distal phalanges of both hands with pointed terminal tufts. Note that the bone density is normal in all the visualized bones (Courtesy of Dr. Sharifah Intan with permission from Radiopaedia.org)

Table 42.3 Imaging pitfalls and differentiating features between pyknodysostosis and cleidocranial dysostosis

Imaging pitfalls	Pyknodysostosis (exclusive features)	Cleidocranial dysostosis (exclusive features)
Widened skull sutures with persistent fontanelles, wormian bones, frontoparietal bossing, platybasia	Short stature	Small and elevated scapulae
Defective dentition sometimes causing dental caries and osteomyelitis of the jaw	Obtuse angle of the mandible	Narrow bell-shaped chest
Hypoplastic clavicles and terminal phalanges	Diffuse osteosclerosis with transverse fractures particularly in the limbs	Pseudo-widening of the pubic symphysis

and late-onset aortic regurgitation (Langer and Carey 1966; Resnick 1994; Mikles and Stanton 1997; Rasalkar et al. 2011; Di Cesare et al. 2012).

Hurler syndrome is a rare autosomal recessive disorder of mucopolysaccharide metabolism (MPS type 1), which is characterized clinically
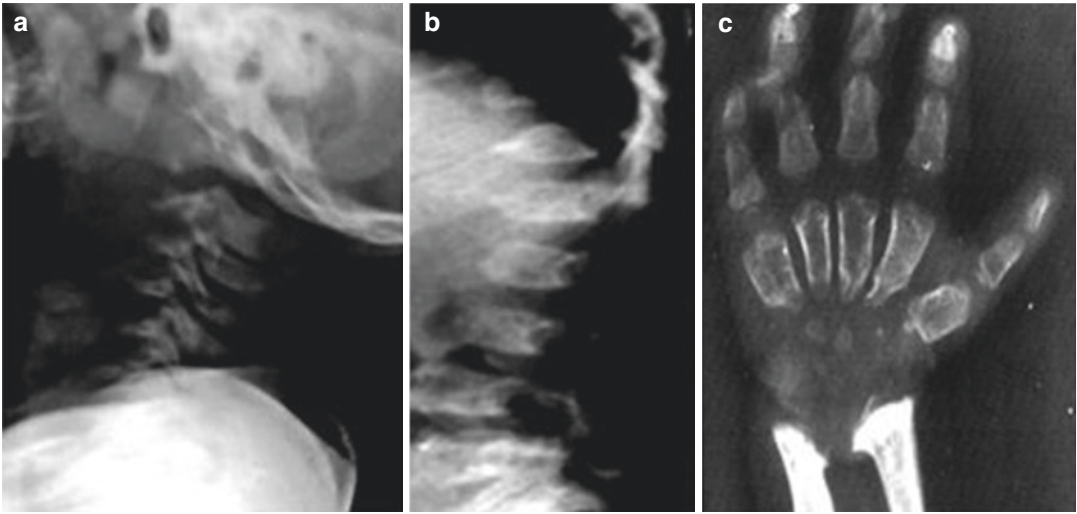
Fig. 42.13 Morquio syndrome. (**a**) Lateral radiograph of the cervical spine shows universal platyspondyly. Hypoplasia of the odontoid process is also noted. Intervertebral disk spaces are normal. (**b**) Lateral thoracolumbar spine radiograph shows platyspondyly with central beaking and posterior scalloping. (**c**) Frontal hand radiograph shows pointed proximal metacarpals with irregular articular ends of the radius and ulna (Reproduced with permission from: Subbarao (2014))
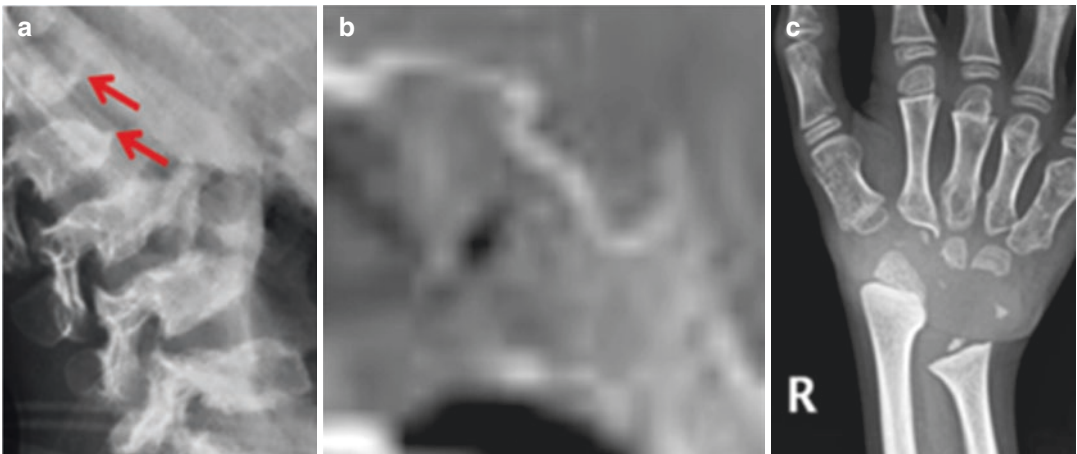

Fig. 42.14 Hurler syndrome. (**a**) Lateral thoracolumbar spine radiograph shows platyspondyly with anteroinferior beaking (*arrows*). (**b**) Sagittal-reconstructed CT image of the sella (bone window) shows a "J"-shaped sella. (**c**) Frontal radiograph of the wrist shows tilting of the ulna toward the radius and bullet-shaped proximal ends of the metacarpals (Reproduced with permission from: Subbarao (2014))

by mental retardation, corneal clouding, deafness, and cardiac disease. Dermatan sulfate and heparin sulfate are the mucopolysaccharides excreted excessively in the urine. The prognosis is poor in most patients, with death in the first decade due to cardiac disease (Rasalkar et al. 2011). The radiographic findings (Fig. 42.14) in the spine consist of hypoplastic vertebra at the thoracolumbar junction, mainly at the anterosuperior aspect with anterior inferior vertebral beaking causing thoracolumbar kyphosis. Atlantoaxial subluxation, proximal metacarpal tapering, short and wide tubular bones, flaring of iliac bones, and coxa vara or valga are also seen

Table 42.4 Imaging pitfalls and differentiating features between Morquio syndrome and Hurler syndrome

Imaging pitfalls	Morquio syndrome (exclusive features)	Hurler syndrome (exclusive features)
Anterior vertebral beaking and posterior vertebral scalloping Hypoplastic vertebra at thoracolumbar junction with thoracolumbar kyphosis Atlantoaxial subluxation Small flared iliac bones Coxa vara or valga Short and wide tubular bones Proximal metacarpal tapering	Universal platyspondyly with anterior central vertebral beaking Pectus carinatum Cardiac abnormalities Normal intelligence	Anterior inferior vertebral beaking Skull changes – macrocephaly, frontal bossing, large J-shaped sella, calvarial thickening, craniosynostosis, hydrocephalus Short thick clavicles Oar-shaped ribs Osteoporosis Hepatosplenomegaly Mental retardation

in the affected patients. However, the differentiating features (Table 42.4) include the presence of macrocephaly, frontal bossing, calvarial thickening, craniosynostosis involving sagittal and lambdoid sutures, hydrocephalus, enlarged J-shaped sella, widening of anterior ribs (oar-shaped/paddle ribs), osteoporosis, and hepatosplenomegaly (Resnick 1994; Rasalkar et al. 2011; Greenspan 2015).

Spondyloepiphyseal dysplasia (SED) refers to hereditary chondrodysplasia characterized by predominant involvement of the spine and epiphysis of the long bones, leading to disproportionate dwarfism. The inheritance is X-linked recessive, autosomal dominant, and autosomal recessive. It has two subtypes, namely, SED congenita and SED tarda. SED tarda is the milder form, which manifests in late childhood or adolescence (Lakhar and Raphael 2003). The cardinal imaging features (Fig. 42.15) include platyspondyly with mounds of dense bone over central and posterior part of vertebral end plates causing hump-shaped vertebra or absence of ossification in the anterior parts of vertebral end plates giving the appearance of anterior vertebral beaking. Thin intervertebral disk spaces, odontoid hypoplasia (seen in SED congenita), flattened and dysplastic epiphysis of long bones (particularly proximal femoral epiphysis), small iliac wings, and kyphoscoliosis are the other important radiographic features (Lakhar and Raphael 2003; Greenspan 2015). Complications include premature osteoarthritis and atlantoaxial subluxation. Morquio syndrome is a close differential due to the presence of diffuse platyspondyly

Fig. 42.15 Spondyloepiphyseal dysplasia tarda. Lateral thoracolumbar spine radiograph shows hyperostotic bone deposited at the posterior two-thirds of the vertebral end plates causing a "hump-shaped" or "heaping up" vertebra (*arrows*) along with the thin disk spaces (Reproduced with permission from: Subbarao (2014))

with hump-shaped vertebra (mimicking anterior vertebral beaking) and presence of dysplastic epiphysis. However, the absence of imaging fea-

tures, namely, anterior central vertebral beaking and posterior scalloping, normal disk height, proximal metacarpal tapering, and systemic manifestations (cardiac and visceral involvement, corneal clouding, and metabolic abnormality), point toward SED (Resnick 1994; Lakhar and Raphael 2003; Greenspan 2015).

42.7 Achondroplasia and Pseudoachondroplasia

Achondroplasia is a short-limb dwarfing dysplasia characterized by abnormal epiphyseal chondroblastic growth and maturation. It occurs due to sporadic mutation in about 80% of the cases, and autosomal dominant transmission occurs in the remaining ones. The enchondral ossification

centers (particularly at the base of the skull and ends of long bones) are involved more than others, and the periosteal and membranous ossification are normal. The disease presents at birth and commonly involves the skull, spine, pelvis, and limbs (Resnick 1994; Subbarao 2014).

The pathognomonic radiographic features (Fig. 42.16) include:

► *Limbs*: Symmetrical rhizomelic limb shortening, widening of the shafts (due to normal periosteal ossification), splaying and cupping of the metaphysis with V-shaped growth plates (chevron sign), short and thick tubular bones of the hands and feet, trident hand (separation of the middle and ring fingers with all fingers of the same length), and delayed appearance of the carpal bones

Fig. 42.16 Skeletal survey in a patient with achondroplasia. (**a**) Lateral skull radiograph shows a large skull with a narrow base. (**b**) Frontal radiograph of the pelvis shows a champagne glass appearance of the pelvic inlet with horizontal acetabular roofs. (**c**) Frontal and (**d**) lateral radiographs of the lumbosacral spine show short thick pedicles with progressive caudal narrowing of the interpedicular distance and lumbar canal stenosis, along with posterior scalloping of vertebrae. The sacrum is oriented horizontally. (**e**) Frontal hand radiograph shows a trident hand with short and stubby phalanges (Reproduced with permission from: Subbarao (2014))

► *Skull*: Large cranium (with short anteroposterior dimension – brachycephaly), small base of the skull often with stenotic foramen magnum (causing cervicomedullary kink), basilar impression, and prominent frontal and small nasal bones

► *Spine*: Posterior vertebral scalloping, bullet-shaped vertebrae, widened intervertebral disk height (due to increased amount of cartilage), progressive caudal narrowing of interpedicular distance in the lumbar spine, short and thick pedicles (causing spinal stenosis), and exaggerated lumbar lordosis with increased angle between the sacrum and lumbar spine (horizontally oriented sacrum)

► *Pelvis*: Small pelvis with champagne glass pelvic inlet, horizontal acetabular roofs, squared (tombstone) iliac wings, and narrow sacrosciatic notches

► *Chest*: Anteroposterior shortening of the ribs with anterior flaring

► Neurological complications are seen in many cases and vary from cervicomedullary compression and hydrocephalus due to small foramen magnum and cord compression due to lumbar canal stenosis (Resnick 1994; Yochum and Rowe 2005; Subbarao 2014).

Pseudoachondroplasia is a rarer and similar skeletal dysplasia which features the rhizomelic type of dwarfism. The inheritance is autosomal dominant in majority of the cases. In contrast to achondroplasia, most patients are normal at birth and present around 2–3 years of age with delay in walking/abnormal waddling gait or lower limb deformity. The most obvious discriminating feature is the presence of normal skull and facial bones and normal facies (Tandon et al. 2008; Radlović et al. 2013; Subbarao 2014). The radiographic changes (Fig. 42.17) are quite similar to achondroplasia, especially in the pelvis and limbs, except that the epiphyses are also involved in limbs, which are small and fragmented with a delayed appearance. Proximal femoral and humeral epiphyses are affected in most cases, with medial beaking of the femoral neck. Spinal features also resemble achondroplasia, but the interpedicular distances are characteristically normal. Therefore, stenosis of the foramen magnum and lumbar canal is not seen. In addition, marked platyspondyly and odontoid dysplasia are the other spinal abnormalities often seen in patients with pseudoachondroplasia exclusively. However, the skull is normal, unlike achondroplasia (Yochum and Rowe 2005; Tandon et al. 2008; Radlović et al. 2013; Subbarao 2014). The pitfalls and differences between achondroplasia and pseudoachondroplasia are summarized in Table 42.5.
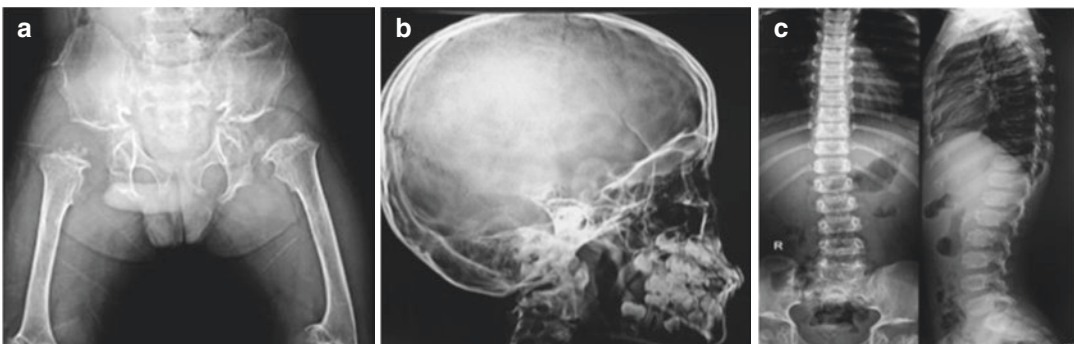

Fig. 42.17 Skeletal survey in a patient with pseudoachondroplasia. (**a**) Frontal radiograph of the pelvis shows a champagne glass pelvic inlet (same as achondroplasia) along with delayed appearance of bilateral proximal femoral epiphysis which are flattened and fragmented. (**b**) Lateral skull radiograph is normal. (**c**) Frontal and (**d**) lateral thoracolumbar spine radiographs show normal interpedicular distances (Reproduced with permission from: Subbarao (2014))

Table 42.5 Imaging pitfalls and differentiating features between achondroplasia and pseudoachondroplasia

Anatomical region	Imaging pitfalls/mimics	Achondroplasia (exclusive features)	Pseudoachondroplasia (exclusive features)
Limbs	Rhizomelic dwarfism with flaring and cupping of the metaphysis	None	Additional involvement of epiphysis (small, fragmented, and delayed appearance)
Spine	Bullet-nose vertebrae, widened disk spaces, posterior vertebral scalloping	Short and thick pedicles, caudal narrowing of interpedicular distance, lumbar canal stenosis	Platyspondyly
Pelvis	Small squared pelvis with champagne glass pelvic inlet and horizontal acetabular roofs	None	None
Skull and facial bones	None	Large cranium with small base of the skull	Normal (Fig. 42.17b)

42.8   Chondrodysplasia Punctata, Multiple Epiphyseal Dysplasia, Meyer Dysplasia, Perthes Disease, and Cretinism

Chondrodysplasia punctata (also known as dysplasia epiphysealis punctata) is a genetically heterogeneous epiphyseal dysplasia characterized by punctate or stippled calcification of multiple epiphyseal centers. It can be classified into several subtypes: the autosomal recessive (rhizomelic type associated with peroxisomal enzyme disorder and death often in the first few years of life) and the X-linked dominant (CDPX2 or Conradi-Hünermann-Happle syndrome). A third rare subtype is the brachytelephalangic type with X-linked recessive inheritance. In addition to genetically inherited forms, chondrodysplasia punctata may also be seen with embryotoxicity due to maternal use of coumarin-like compounds or phenytoin during gestation, or babies born to mothers with autoimmune diseases like systemic lupus erythematosus. It is important to identify the radiological type in order to prognosticate the patient. Punctate calcifications tend to disappear after the first year of life, thus necessitating early diagnosis (Morthy et al. 2002; Figueirêdo et al. 2007; Irving et al. 2008). Radiological features of the rhizomelic and Conradi-Hünermann subtypes

(Fig. 42.18) of chondrodysplasia punctata are tabulated in Table 42.6.

Multiple epiphyseal dysplasia (also known as *dysplasia epiphysealis multiplex or Fairbank-Ribbing disease*) is a genetically heterogeneous skeletal dysplasia caused by mutations in at least six genes, characterized by flattening and fragmentation of epiphyses. The transmission is autosomal dominant in most of the cases (Unger et al. 2008; Panda et al. 2014). Unlike chondrodysplasia punctata, multiple epiphyseal dysplasia presents in older children (after 2–4 years of age, when the child begins to walk) with complaints of waddling gait and difficulty in running. Short stature is not a feature. The radiographic features (Fig. 42.19) include bilateral symmetrical involvement of epiphysis of the hips, knees, ankles and, less commonly, the shoulders, wrists, hands, and feet which are flattened and fragmented (with hypoplastic femoral and tibial condyles with shallow intercondylar notch). In contrast, the stippling in chondrodysplasia punctata is finer than the fragmentation seen in multiple epiphyseal dysplasia. The lateral tibiotalar slant (due to thinning of lateral tibial epiphysis) and double-layered patella are the other differentiating features. The involvement of the spine is uncommon and, if it occurs, is mild with features including mild endplate irregularity, anterior wedging, multiple Schmorl nodes (like
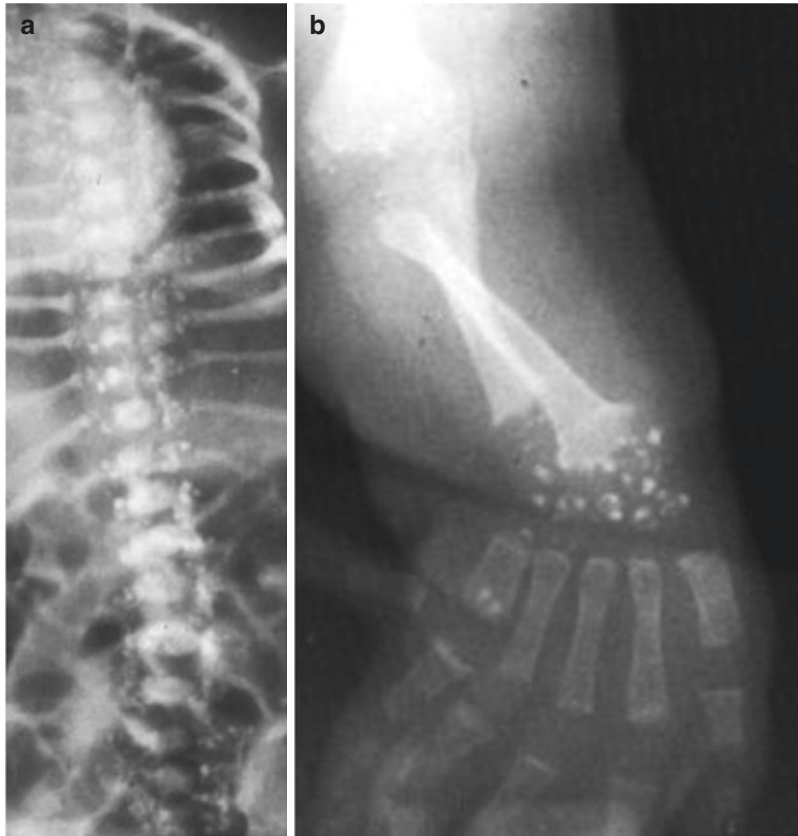
Fig. 42.18 Chondrodysplasia punctata (Conradi-Hünermann subtype). (**a**) Frontal radiograph of the thoracolumbar spine shows punctate calcifications adjacent to vertebrae with vertebral deformities. (**b**) Radiograph of the forearm shows stippling of the wrist (Reproduced with permission from: Subbarao (2014))

Table 42.6 Imaging features of the rhizomelic and Conradi-Hünermann subtypes of chondrodysplasia punctata

Rhizomelic type (lethal+ mental retardation +)	Conradi-Hünermann type (normal intelligence and life span)
Epiphyseal stippling noted mainly in large joints, such as the hips, shoulders, knee, and wrists	Stippling at ends of long bones as well as short tubular bones in the hands and feet
Short tubular bones in the hands and foot spared	Metaphyses and diaphyses are normal
Metaphyses are often flared	Occasional asymmetric limb shortening
Symmetrical rhizomelic limb shortening	Stippling in the spine present
Stippling in the spine absent (coronal clefts in vertebrae are present)	Stippling may also involve ends of ribs, hyoid bone, thyroid cartilage, larynx and trachea, and base of the skull

in Scheuermann disease), and scoliosis with absent platyspondyly. Dens agenesis is also seen in some cases causing atlantoaxial subluxation. Complications include premature degenerative changes, slipped capital femoral epiphysis, and osteochondritis dissecans (Unger et al. 2008; Panda et al. 2014).

Legg-Calve-Perthes disease, Meyer dysplasia, and *cretinism* can have similar radiographic features as multiple epiphyseal dysplasia. However, the symmetrical nature, involvement of characteristic joints, and absence of other systemic features are helpful in differentiating points that favor multiple epiphyseal dysplasia. Legg-Calve-Perthes disease (osteonecrosis of proximal femoral epiphysis) can be bilateral in 10–15% of cases; however, it is more often sequential rather than simultaneous. Bilateral symmetrical involvement favors epiphyseal dysplasia. Meyer dysplasia is a subtype
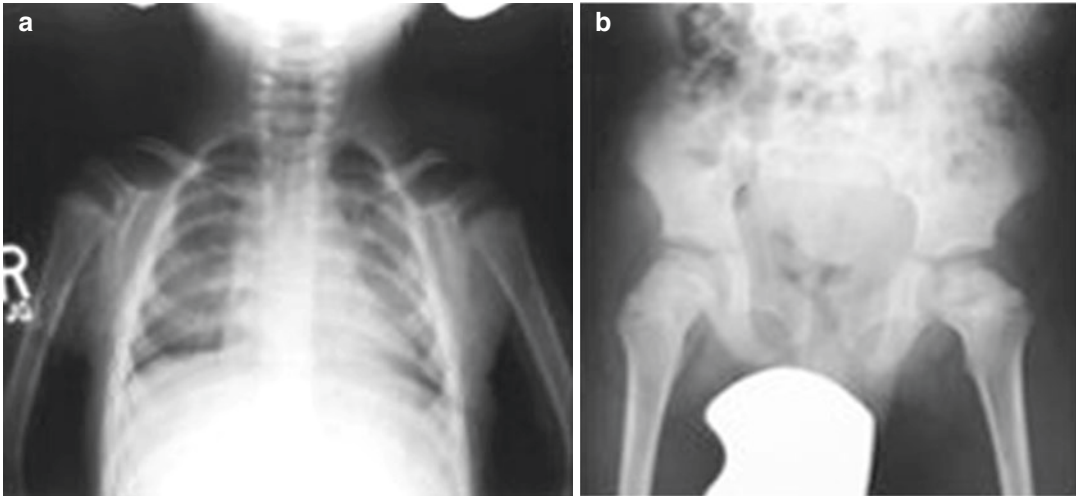
Fig. 42.19 Multiple epiphyseal dysplasia. (**a**) Frontal chest radiograph shows the absence of proximal humeral ossification centers. (**b**) Frontal radiograph of the pelvis shows symmetrical flattening of bilateral proximal femo-ral epiphysis (Courtesy of Professor L Das Narla, Virginia Commonwealth University Medical Center, Richmond, USA)

of epiphyseal dysplasia confined to the hips, which is often asymptomatic or has milder symptoms, unlike Legg-Calve-Perthes disease. The absence of involvement of other epiphysis differentiates Meyer dysplasia from multiple epiphyseal dysplasia. Cretinism (congenital hypothyroidism) shows fragmented and dysplastic epiphysis, with delayed bone age. The spine is also involved in some cases, causing anterior vertebral beaking. Therefore, delayed skeletal maturation, the presence of other systemic features and proper clinical history, along with hormonal assays, distinguish it from multiple epiphyseal dysplasia (Yochum and Rowe 2005; Panda et al. 2014).

42.9 Metaphyseal Chondrodysplasia (Schmid Type) and Rickets

Schmid-type metaphyseal chondrodysplasia is a rare autosomal dominant disorder characterized by moderately short stature with short limbs, bowing of long bones, waddling gait, and coxa vara. It is caused by mutations in the COL10A1 (6q21-q22) gene encoding the collagen alpha-1(X) chain. *Spahr-type metaphyseal chondrodysplasia* is a similar condition which is autosomal recessive and presents with moderate short stature. It is due to MMP 13 mutations which cause disruption of a crucial hydrogen bond in the calcium-binding region of the catalytic domain of the matrix metalloproteinase. Molecular confirmation is required for distinction of both the conditions. Patients often present in second to third year of life (Lachman et al. 1988; Elliott et al. 2005; Mäkitie et al. 2005). The radiographic changes (Fig. 42.20) are similar to those of *rickets* (particularly *nutritional rickets*) (Fig. 42.21) and consist of cupping, flaring, and fraying of the metaphysis with widening of the growth plate (most pronounced at the knees); coxa vara; bowing of long bones (commonly femur); enlarged capital femoral epiphysis in early childhood; cupping, splaying, and sclerosis of the anterior aspect of the ribs; and a normal spine. Positive family history and no abnormality in biochemical analysis (serum calcium, phosphate, parathyroid hormone, and alkaline phosphatase levels) help in differentiating metaphyseal chondrodysplasias from rickets. Rickets is a metabolic bone disease which is due to deficiency in one or more of calcium, phosphorus, and 1,25 di-hydroxy vitamin D (Lachman et al. 1988; Dahl and Birkebaek 1996; Elliott et al. 2005; Mäkitie et al. 2005; Bonafé et al. 2014).
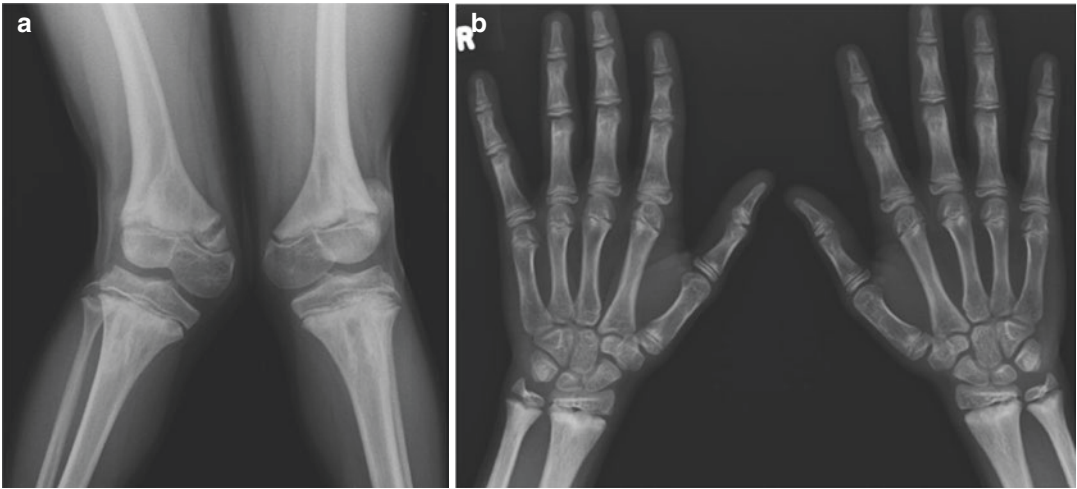
Fig. 42.20 Metaphyseal dysplasia (Schmid type). Frontal radiographs of (**a**) both knees and (**b**) both wrists show expansion, sclerosis, and irregularity of the metaphyses of the femurs, tibiae, radii, and ulnae bilaterally, with widened growth plates

Fig. 42.21 Frontal radiograph of the left wrist in a patient with rickets shows cupping, splaying, and fraying of the distal metaphysis of the left radius and ulna, with widened growth plates

42.10 Camurati-Engelmann Disease, Ghosal-Type Hemato-Diaphyseal Dysplasia, Ribbing Disease, Caffey Disease, Intramedullary Osteosclerosis, and Erdheim-Chester Disease

Camurati-Engelmann disease (also known as *Engelmann disease* or *progressive diaphyseal dysplasia*) is a rare autosomal dominant sclerosing bony dysplasia characterized by bilateral, symmetrical, fusiform thickening of the cortical bone in the diaphysis of long tubular bones (Fig. 42.22). Engelmann disease affects long bones and bones formed by intramembranous ossification; therefore, calvarial hyperostosis is also as frequently seen as the involvement of long bones. The disorder manifests in the first decade of life with symptoms of bone and muscle pain, weakness and atrophy, waddling and broad-based gait, and delayed puberty. It is more common in boys (Vanhoenacker et al. 2003; Bartuseviciene et al. 2009; Damiá Ade et al. 2010).

Ghosal hemato-diaphyseal dysplasia is a similar autosomal recessive disorder which features metadiaphyseal dysplasia of long bones and

Fig. 42.22 Engelmann disease. Frontal radiograph of the pelvis and both femurs shows symmetrical cortical thickening involving the diaphysis of both femurs (Reproduced with permission from: Subbarao (2013))

Fig. 42.23 Ribbing disease. Frontal radiograph of both legs shows asymmetrical cortical thickening of the diaphysis of both tibiae (left > right) (Reproduced with permission from: Damle et al. (2011))

hematologic abnormalities due to fibrosis or sclerosis of the bone marrow. The differentiating features from Engelmann disease include involvement of both metaphysis and diaphysis of long bones (unlike only diaphyseal involvement in Engelmann disease), presence of defective hematopoiesis, absence of gait abnormalities, elevated levels of immunoglobulins, and autosomal recessive mode of inheritance (in contrast to autosomal dominant in Engelmann disease) (Arora et al. 2015).

Ribbing disease (also known as *hereditary multiple diaphyseal sclerosis*) is another rare sclerosing dysplasia which closely resembles Engelmann disease and is characterized by benign endosteal and periosteal new bone formation confined to the diaphysis of the long bones of the lower extremities (Fig. 42.23). However, unlike Engelmann disease, it is of autosomal

recessive inheritance (with no gender predominance) and presents later in life (after puberty) with just pain in the involved extremity. It is either unilateral or asymmetrically and asynchronously bilateral (unlike bilateral symmetrical involvement of the former two disorders). There is no involvement of the skull and hematological abnormalities are not seen. Histologically, Ribbing disease shows isolated osteoblastic activity with progressive obstruction of the haversian systems, whereas Engelmann disease features both osteoblastic and osteoclastic activity, implying bone formation and resorption with trabecular thickening and normal or enlarged haversian systems. Some authors have proposed that both entities represent phenotypic variations of the same disorder (Seeger et al. 1996; Damle et al. 2011; Oztürkmen and Karamehmetoğlu 2011).

Caffey disease (also known as *infantile cortical hyperostosis*) is a largely self-limiting inher-

ited disorder with both autosomal dominant and recessive inheritances (sporadic cases also seen infrequently). It is characterized by a clinical triad of (1) presentation within first 6 months of life; (2) hyperirritability, bony lesions, and soft tissue swelling; and (3) mandibular involvement. Other sites of involvement include the ulna, clavicle, and, less commonly, other long bones, scapula, ribs, and skull. Radiological findings (Fig. 42.24) include lamellated periosteal reactions with cortical thickening and soft tissue swelling involving the diaphysis. It often resolves spontaneously within 6 months to 1 year (Kutty et al. 2010; Panda et al. 2014).

Intramedullary osteosclerosis is a nonhereditary condition that mimics Ribbing disease and is characterized by unilateral or asymmetrical, intramedullary diaphyseal osteosclerosis of one or more long bones of one or both lower extremities. There is no periosteal new bone formation and soft tissue involvement, with onset in adulthood. However, female predominance, lack of family history, and medullary sclerosis as the dominant imaging findings differentiate between the two disorders (Chanchairujira et al. 2001).

Erdheim-Chester disease is a rare nonfamilial, non-Langerhans cell lipogranulomatous disorder with infiltration by lipid-laden histiocytes, Touton giant cells, and variable amount of fibrosis. It often presents in middle age, with a slight male predominance. It is a multisystem disorder, and its manifestations include musculoskeletal involvement (most common), diabetes insipidus, exophthalmos (due to retro-orbital involvement), and involvement of the lungs and kidneys. Like Engelmann disease, it shows bilateral symmetrical metadiaphyseal osteosclerosis with cortical thickening (Fig. 42.25). However, onset in adulthood with absent family history, multisystem involvement, moderate anemia, elevated erythrocyte sedimentation rate and C-reactive protein, abnormal lipid metabolism, sparing of axial skeleton, and partial epiphyseal involvement with bone infarcts (in some cases) are the contrasting points (Dion et al. 2006).

Fig. 42.24 Caffey disease. Frontal radiograph of the left femur and knee in an 8-month-old boy shows lamellated periosteal reaction involving the diaphysis of the femur with soft tissue swelling

42.11 Osteopoikilosis and Sclerotic Metastases

Osteopoikilosis is a rare autosomal dominant sclerosing dysplasia characterized by multiple small (1–10 mm), symmetrical, uniform, sclerotic, ovoid opacities (bone islands) parallel to surrounding trabeculae and clustered around joints (Fig. 42.26). The common sites of
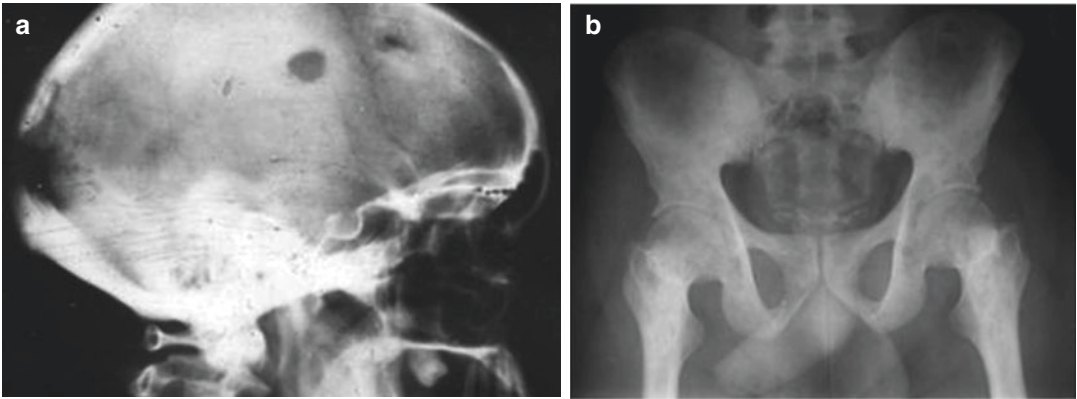
Fig. 42.25 Erdheim-Chester disease. (**a**) Lateral radiograph of the skull shows a well-defined rounded radiolucent lesion with beveled edges in the parietal bone, with another similar lesion also noted in the frontal bone. (**b**) Frontal radiograph of the pelvis and hips shows symmetrical metadiaphyseal sclerosis involving both proximal femurs. Patchy areas of sclerosis and radiolucency are also seen involving both pelvic bones

Fig. 42.26 Osteopoikilosis. Frontal radiograph of the pelvis shows multiple, bilateral symmetrical, sclerotic lesions of uniform size around both hip joints (Reproduced with permission from: Subbarao (2013))

involvement include ends of long bones, carpals, tarsals, and peri-acetabular and subglenoid areas. The spine, skull, and ribs are involved rarely. They often develop in childhood and do not regress (so are seen in all age groups). It often coexists with osteopathia striata and melorheostosis. They do not demonstrate increased uptake on bone scintigraphy and have no malignant potential (Benli et al. 1992; Stacy et al. 2002; Karwar et al. 2005).

Fig. 42.27 Frontal radiograph of the pelvis shows multiple sclerotic foci of variable sizes involving the pelvic bones and proximal femurs bilaterally, with variable distribution in a patient with osteoblastic metastasis from prostate carcinoma. Left hip implant is noted (Courtesy of Dr. Stefan Ludwig with permission from Radiopaedia. org)

Sclerotic metastases are an important differential and can be differentiated by the variable size and distribution of the lesions (Fig. 42.27). Additionally, they show increased uptake on bone scintigraphy (Stacy et al. 2002; Karwar et al. 2005; Panda et al. 2014).

Conclusion

Imaging enables the correct diagnosis of skeletal dysplasias and their distinction from other dysplastic and non-dysplastic conditions. This would help in targeted workup and prevent unnecessary investigations. An accurate diagnosis of these complex abnormalities is also essential for their early management, assessment of prognosis, and genetic counseling.

References

Ablin D, Greenspan A, Reinhart M, Grix A (1990) Differentiation of child abuse from osteogenesis imperfecta. AJR Am J Roentgenol 154:1035–1046

Arora R, Aggarwal S, Deme S (2015) Ghosal hematodiaphyseal dysplasia – a concise review including an illustrative patient. Skeletal Radiol 44:447–450

Bartuseviciene A, Samuilis A, Skucas J (2009) Camurati-Engelmann disease imaging: clinical features and differential diagnosis. Skeletal Radiol 38:1037–1043

Bathi RJ, Masur VN (2000) Pyknodysostosis – a report of two cases with a brief review of the literature. Int J Oral Maxillofac Surg 29:439–442

Baujat G, Le Merrer M (2007) Ellis-van Creveld syndrome. Orphanet J Rare Dis 2:27

Benli IT, Akalin S, Boysan E et al (1992) Epidemiological, clinical and radiological aspects of osteopoikilosis. J Bone Joint Surg Br 74:504–506

Bonafé L, Liang J, Gorna MW et al (2014) MMP13 mutations are the cause of recessive metaphyseal dysplasia, Spahr type. Am J Med Genet A 164:1175–1179

Chanchairujira K, Chung CB, Lai YM et al (2001) Intramedullary osteosclerosis: imaging features in nine patients. Radiology 220:225–230

Chauss J (1955) Chondroectodermal dysplasia (Ellis van Creveld disease) 1. Radiology 65:213–217

Dahl M, Birkebaek NH (1996) Metaphyseal chondrodysplasia as differential diagnosis to rickets. Ugeskr Laeger 158:1683–1684

Damiá Ade B, Morón CC, Pérez PA et al (2010) Bone scintigraphy in Engelmann-Camurati disease. Clin Nucl Med 35:559–560

Damle NA, Patnecha M, Kumar P et al (2011) Ribbing disease: uncommon cause of a common symptom. Indian J Nucl Med 26:36–39

De Vries J, Yntema J, van Die C et al (2009) Jeune syndrome: description of 13 cases and a proposal for follow-up protocol. Eur J Pediatr 169:77–88

Di Cesare A, Di Cagno A, Moffa S et al (2012) A description of skeletal manifestation in adult case of Morquio syndrome: radiographic and MRI appearance. Case Rep Med 2012:1–6

Dion E, Graef C, Miquel A et al (2006) Bone involvement in Erdheim-Chester disease: imaging findings including periostitis and partial epiphyseal involvement. Radiology 238:632–639

Elliott AM, Field FM, Rimoin DL et al (2005) Hand involvement in Schmid metaphyseal chondrodysplasia. Am J Med Genet A 132:191–193

Figueirêdo SDS, Araújo JS, Kozan JEM et al (2007) Rhizomelic chondrodysplasia punctata: a case report and brief literature review. Radiol Bras 40:69–72

Greenspan A (2015) Orthopedic imaging: a practical approach, 6th edn. Lippincott Williams & Wilkins, Philadelphia

Grover SB, Kumar S, Taneja DK (2003) Radiological quiz- skeletal radiology. Indian J Radiol Imaging 13:335–338

Imerci A, Canbek U, Haghari S, Sürer L, Kocak M (2015) Idiopathic juvenile osteoporosis: a case report and review of the literature. Int J Surg Case Rep 9:127–129

Irving MD, Chitty LS, Mansour S et al (2008) Chondrodysplasia punctata: a clinical diagnostic and radiological review. Clin Dysmorphol 17:229–241

Kapur R (2007) Achondrogenesis. Pediatr Dev Pathol 10:253–255

Karwar J, Gupta R, Sharma G (2005) Osteopoikilosis: a case report. Indian J Radiol Imaging 15:453–454

Keats T, Riddervold H, Michaelis L (1970) Thanatophoric dwarfism. AJR Am J Roentgenol 108:473–480

Kozlowski K, Prokop E, Zybaczynski J (1970) Thanatophoric dwarfism. Br J Radiol 43:565–568

Kutty N, Thomas D, George L et al (2010) Caffey disease or infantile cortical hyperostosis: a case report. Oman Med J 25:134–136

Lachman RS, Rimoin DL, Spranger J (1988) Metaphyseal chondrodysplasia, Schmid type. Clinical and radiographic delineation with a review of the literature. Pediatr Radiol 18:93–102

Lakhar BN, Raphael R (2003) Spondyloepiphyseal dysplasia: an evaluation of six cases. Indian J Radiol Imaging 13:199–203

Langer LO, Carey LS (1966) The roentgenographic features of the Ks mucopolysaccharidosis of Morquio (Morquio-Brailsford's disease). AJR Am J Roentgenol 97:1–20

Machado CDV, Siquara Da Rocha MCB, Telles PDDS et al (2015) Infantile osteopetrosis associated with osteomyelitis. BMJ Case Rep pii: bcr2014208085

Mäkitie O, Susic M, Ward L et al (2005) Schmid type of metaphyseal chondrodysplasia and COL10A1 mutations-findings in 10 patients. Am J Med Genet A 137:241–248

Mikles M, Stanton RP (1997) A review of Morquio syndrome. Am J Orthop 26:533–540

Miller E, Blaser S, Shannon P, Widjaja E (2009) Brain and bone abnormalities of thanatophoric dwarfism. AJR Am J Roentgenol 192:48–51

Morthy NL, Venkataratnam I, Rao RP et al (2002) Images: chondrodysplasia punctata. Indian J Radiol Imaging 12:397–398

Oztürkmen Y, Karamehmetoğlu M (2011) Ribbing disease: a case report and literature review. Acta Orthop Traumatol Turc 45:58–65

Panda A, Gamanagatti S, Jana M et al (2014) Skeletal dysplasias: a radiographic approach and review of common non-lethal skeletal dysplasias. World J Radiol 6:808–825

Radlović V, Smoljanić Z, Radlović N et al (2013) Pseudoachondroplasia: a case report. Srp Arh Celok Lek 141:676–679

Rasalkar DD, Chu WCW, Hui J et al (2011) Pictorial review of mucopolysaccharidosis with emphasis on MRI features of brain and spine. Br J Radiol 84:469–477

Rasmussen S, Bieber F, Benacerraf B et al (1996) Epidemiology of osteochondrodysplasias: changing trends due to advances in prenatal diagnosis. Am J Med Genet 61:49–58

Renaud A, Aucourt J, Weill J et al (2013) Radiographic features of osteogenesis imperfecta. Insights Imaging 4:417–429

Resnick D (1994) Diagnosis of bone and joint disorders, 4th edn. Saunders, Philadelphia

Seeger LL, Hewel KC, Yao L et al (1996) Ribbing disease (multiple diaphyseal sclerosis): imaging and differential diagnosis. AJR Am J Roentgenol 167:689–694

Shen Z, Zou CC, Yang RW, Zhao ZY (2009) Cleidocranial dysplasia: report of 3 cases and literature review. Clin Pediatr 48:194–198

Stacy GS, Heck RK, Peabody TD et al (2002) Neoplastic and tumor like lesions detected on MR imaging of the knee in patients with suspected internal derangement: part I, intraosseous entities. AJR Am J Roentgenol 178:589–594

Subbarao K (2013) Skeletal dysplasia (sclerosing dysplasias) Part I. NJR 3:1–10

Subbarao K (2014) Non-sclerosing skeletal dysplasias. NJR 4:1–11

Tandon A, Bhargava SK, Goel S et al (2008) Pseudoachondroplasia: a rare cause of rhizomelic dwarfism. Indian J Orthop 42:477–479

Thakkar P, Aiyer S, Shah B (2012) Asphyxiating thoracic dystrophy (Jeune syndrome). JCR 2012:15–17

Tüysüz B, Barış S, Aksoy F, Madazlı R, Üngür S, Sever L (2009) Clinical variability of asphyxiating thoracic dystrophy (Jeune) syndrome: evaluation and classification of 13 patients. Am J Med Genet A 149:1727–1733

Unger S, Bonafé L, Superti-Furga A (2008) Multiple epiphyseal dysplasia: clinical and radiographic features, differential diagnosis and molecular basis. Best Pract Res Clin Rheumatol 22:19–32

Vanhoenacker FM, Janssens K, Van Hul W et al (2003) Camurati-Engelmann disease. Review of radioclinical features. Acta Radiol 44:430–434

Warman M, Cormier Daire V, Hall C et al (2011) Nosology and classification of genetic skeletal disorders 2010 revision. Am J Med Genet A 155:943–968

Weiner D, Jonah D, Leighley B et al (2013) Orthopaedic manifestations of chondroectodermal dysplasia the Ellis–van Creveld syndrome. J Child Orthop 7: 465–476

Yochum TR, Rowe LJ (2005) Yochum and Rowe's essentials of skeletal radiology, 3rd edn. Lippincott Williams & Wilkins, Baltimore